ELSEVIER

Ceramics International 27 (2001) 351–361

CERAMICS
INTERNATIONAL

www.elsevier.com/locate/ceramint

Sintering behaviour of ammonium exchanged low silica zeolites synthesised by two different routes

Sathy Chandrasekhar *, P.N. Pramada

Regional Research Laboratory (CSIR), Thiruvananthapuram-695 019, India

Received 11 April 2000; received in revised form 23 April 2000; accepted 21 July 2000

Abstract

Zeolites have been reported as novel precursors for aluminosilicate based ceramics. Even though the zeolites are conventionally synthesised from sodium aluminosilicate gel (gel route), kaolin is found to be an ideal raw material for the synthesis of low silica zeolites (clay route). The small amounts of ancillary minerals present in kaolin may affect the ion exchange and sintering behaviour of these zeolites. The present paper deals with the ammonium exchange of zeolites Na*A* and Na*X* synthesised by these two different routes and the sintering behaviour of these exchanged zeolites at different temperatures was studied by measuring the properties of the sintered products. The influence of the type of zeolite and the method of zeolite synthesis on the sintering behaviour of the exchanged zeolites was examined. The breakdown of zeolite structure was observed at a lower temperature for the gel route zeolites compared to the corresponding clay route zeolites. The final product of sintering in all cases was found to be a mullite–glass composite. Zero water absorption is achieved at a lower temperature of firing for zeolite NH_4X compared to the zeolite NH_4A. X-ray diffraction, thermal analysis and electron microscopic studies substantiated these findings. © 2001 Elsevier Science Ltd and Techna S.r.l. All rights reserved.

Keywords: A. Sintering; B. X-ray methods; C. Thermal properties; D. Mullite; Ceramic precursors

1. Introduction

Zeolites are crystalline aluminosilicates with uniform pores, channels and cavities and have tremendous industrial applications due to their special properties like ion exchange, sorption and catalytic activity. Structurally they are "framework" alumniosilicates which are based on an infinitely extending three dimensional network of AlO_4 and SiO_4 tetrahedra linked to each other by sharing all of their oxygens. The negative charge on AlO_4 is compensated by cations like sodium. The typical unit cell contents of low silica zeolites Na*A* and Na*X* can be represented as $Na_{12}(AlO_2)_{12}(SiO_2)_{12}\cdot 27H_2O$ (Si/Al ratio ~1) and $Na_{86}(AlO_2)_{86}(SiO_2)_{106}\cdot 264H_2O$ (Si/Al ~1.2) respectively. These zeolites differ essentially in the type of polyhedral cages of which they are made of and the sizes of the free apertures of the main channels i.e. 4.2Å for zeolite Na*A* and 7.4Å for zeolite Na*X*. Zeolite Na*A* has no mineral relative whereas zeolite Na*X* is similar to the natural mineral faujasite in the framework structure [1].

Recently, zeolites have been reported as novel precursors for various aluminosilicate ceramics. The zeolites exchanged with various cations can act as precursors for different types of ceramics. Traditionally, ceramics are prepared from naturally-occurring materials like kaolin, feldspar and other silicates or from oxide mixtures with precise chemical and phase composition or by sol–gel method. Zeolites as ceramic precursors have certain advantages which have been discussed in earlier publications by different research groups. A series of studies has been carried out on zeolite based ceramics and commercially available zeolites synthesised by the conventional gel route have been used for the same [2–16].

Low silica zeolites (Si/Al 1–1.5) are generally synthesised from sodium aluminosilicate gel prepared from various silica and alumina sources. Kaolinite has been reported as an ideal combined source for silica and alumina for their synthesis as early as 1964 [1]. The zeolites from kaolinites are always contaminated with trace amounts Fe, Ti, Ca, Mg, etc. which are originally present as ancillary minerals in the naturally-occurring kaolin. Even though processing of the raw clay improves the quality of the

---

* Corresponding author. Tel.: +91-471-490674; fax: 94-471-491712.
E-mail address: sathy@csrrltrd.ren.nic.in (S. Chandrasekhar).

PII: S0272-8842(00)00087-0

clay to some extent, traces of these impurities still remain in the zeolite either in the structure or as associated ions. There is a possibility that the ion exchange and sintering behaviour of these zeolites and the properties of the sintered products may get influenced by these impurities. Recently, calcium exchange of low silica zeolites synthesised by clay route and their sintering behaviour at various temperatures have been reported from our laboratory [17].

The present paper deals with a systematic study on the ammonium ion exchange of zeolites Na*A* and Na*X* prepared by clay and gel routes, sintering of these modified zeolites at various temperatures, measurement of properties of the sintered products and comparison of the sintering behaviour with respect to the type of zeolite as well as the synthesis route.

2. Experimental

2.1. Synthesis of zeolites

A coating grade kaolin supplied by M/s English Indian Clays Ltd, Thiruvananthapuram, India was used as the raw material for the synthesis of zeolites Na*A* and Na*X* by clay route. A sodium aluminium silicate gel prepared by mixing calculated amounts of sodium aluminate, sodium silicate and sodium hydroxide was hydrothermally treated to get the zeolites by gel route. The details have been given elsewhere [18–21].

2.2. Ion exchange of zeolites

The zeolites Na*A* and Na*X* synthesised by the two routes were exchanged with ammonium ions by conventional method. Nearly 10 g of the zeolite was added to 100 ml of 10% ammonium nitrate solution and stirred for 8 h. Then the slurry was kept for about 16 h, centrifuged, the supernatant liquid was decanted and the solids were again treated with a fresh solution of ammonium nitrate in a similar manner. This experiment was repeated five times to ensure that maximum ion exchange has taken place. The ion exchanged zeolites NH_4A and NH_4X thus prepared, were filtered, washed thoroughly and dried. Estimation of sodium in the ion exchanged product was carried out to find the extent of ion exchange.

2.3. Sintering

The ion exchanged zeolites were pressed into thin (1.5 mm thickness) and thick (20 mm thickness) pellets of 10 mm diameter under 125 MPa pressure and heated in a programmable furnace at temperatures 750, 850, 950, 1050 and 1150°C at a rate of 3°C/min with a holding time of 3 h.

2.4. Characterisation

The kaolin, the zeolites, the ammonium exchanged forms and the sintered products were characterised by various methods including chemical, X-ray diffraction (XRD) and thermal analysis. Particle size distribution of the kaolin and zeolites has also been determined. The characterisation of the sintered products include measurement of water absorption, shrinkage, true density, compressive strength, dielectric constant, volume resistivity and dielectric loss. The morphology of selected samples were examined under the scanning electron microscope.

2.4.1. Chemical analysis

Standard wet chemical analysis along with instrumental methods were adopted [22]. SiO_2 was estimated gravimetrically, Al_2O_3, CaO and MgO by complexometry, Fe_2O_3 and TiO_2 by spectrophotometry and Na_2O by flame photometry.

2.4.2. X-ray diffraction analysis

Powder XRD patterns were recorded on a Philips PW 1710 X-ray diffractometer with Ni filtered CuK_α-radiation.

2.4.3. Particle size distribution analysis

Micromeritics sedigraph 5100 particle size analyser was used for determining the size distribution in the samples.

2.4.4. Thermal analysis

Differential thermal analysis (DTA) and Thermogravimetric analysis (TGA) of the ion exchanged zeolites were carried out in a Shimadzu thermal analyser by heating the powdered samples at a rate of 40°C/min. The powdered samples were compacted under a load of 1.5 tons to get pellets of 6 mm diameter and 10 mm length and the shrinkage/expansion was measured in a Thermo-mechanical analyser (TMA) 50 MHz, by heating them at a rate of 100°C/min from 30 to 1000°C.

2.4.5. Physical and mechanical properties

Water absorption, shrinkage, density and compressive strength of the pellets sintered at various temperatures were measured following standard methods [23,24].

2.4.6. Dielectric properties

The dielectric properties such as dielectric constant, resistivity and loss factor of the sintered thin pellets were measured at 1 MHz using a Hewlett-Packard 4192A LF impedance analyser. Gold electrodes were sputtered on to the flat surface of the pellets and the capacitance was measured. The dielectric constant K is calculated from the formula $K=(C\times t)/(\varepsilon_0\times A)$ wherein C is the capacitance, t is the thickness of the sample, ε_0 is the permittivity constant and A is the area of the electrode. The resistance was measured and the resistivity (ρ) is calculated as $\rho = RA/t$ where R is the resistance, A is the area of the electrode surface and t is the thickness of the sample. The loss factor (tan δ) was measured directly from the instrument.

2.4.7. Morphology

A scanning electron microscope, JEOL JSM 5600 LV was used for studying the morphology of the fractured surface of selected fired samples.

3. Results

3.1. Kaolin and the zeolites

The properties of the kaolin and the zeolites Na*A* and Na*X* synthesised by the clay route (CR) and gel route (GR) are given in Table 1. The chemical analyses show that most of the impurity metal ions in the clay are retained in the CR zeolites. The Si/Al ratios of the kaolin as well as the zeolite Na*A* are almost the same whereas zeolite Na*X* has a higher ratio.

The particle size distribution analysis show that the kaolin particles are mostly ultrafine (< 2 μm) in nature. However, the metakaolinisation results in aggregation of these fine particles. The hydrothermal reaction under stirred conditions give CR zeolite Na*A* with a narrow size distribution (2–10 μm). All other zeolites which were synthesised under static condition were found to have a wider particle size range.

The X-ray diffraction analysis of the clay indicates the high kaolinite content with minor quantities of quartz and mica.

3.2. Ion exchanged zeolites

The X-ray diffractograms of the zeolites and their corresponding ammonium exchanged forms are almost identical irrespective of the synthesis routes indicating that no structural change is taking place during the ion exchange. The peak data of the CR and GR zeolites and their ammonium exchanged forms correspond to the standard values for zeolites Na*A* and Na*X* [25]. The chemical assay of the ammonium zeolites are given in Table 2. The ammonium ions have not been estimated and the extent of ion exchange has been found out from the percentage of sodium in the zeolites. Other chemical constituents in the ion exchanged zeolites do not differ much from the original zeolites.

The TG curve of the ammonium exchanged zeolites indicate a higher loss in weight compared to that of the sodium forms (Table 1). The DTA patterns of the ammonium zeolites CR and GR are found to be almost similar (Fig. 1a–d). Two exotherms at 325–400°C and 995–1040°C and one endotherm at 100–185°C are clearly observed for all the four samples and a very small exotherm is also found at ~910°C for CR zeolite NH_4X. In general, the endotherms and exotherms are found to be sharper for zeolite NH_4A.

The TMA curves of the NH_4A and NH_4X zeolites are found to be quite similar in nature. Gradual shrinkage is

Table 1
Properties of kaolin and the zeolites

		CR zeolites[a]		GR zeolites[b]	
Property (%)	Kaolin	Na*A*	Na*X*	Na*A*	Na*X*
SiO_2	45.90	28.68	34.01	28.97	33.43
Al_2O_3	38.90	24.92	23.46	21.11	22.78
Fe_2O_3	0.56	0.48	0.35	0.20	0.15
TiO_2	0.64	0.73	0.78	0.05	0.05
Na_2O	0.08	12.61	12.03	12.81	10.78
Loss on ignition	13.80	22.29	21.57	25.82	26.56
Si/Al	1.00	0.98	1.23	1.17	1.24
Mineralogy (XRD)	Kaolinite, quartz and mica	Zeolite Na*A*	Zeolite Na*X*	Zeolite Na*A*	Zeolite Na*X*
Particle size distribution (μm)					
> 45	0.80	0.98	32.14	47.00	29.00
< 45 > 10	2.50	1.24	14.43	11.26	10.65
< 10 > 2	16.70	96.54	50.90	39.75	57.69
< 2	80.00	1.24	2.55	1.99	2.66

[a] CR — clay route.
[b] GR — gel route.

Table 2
Chemical assay of the ammonium exchanged zeolites

	CR zeolites[a]		GR zeolites[b]	
Constituents (%)	NH_4A	NH_4X	NH_4A	NH_4X
SiO_2	29.81	36.48	29.82	44.09
Al_2O_3	25.31	23.03	22.81	28.07
Fe_2O_3	0.50	0.56	0.25	0.16
TiO_2	0.80	0.82	0.05	0.05
Na_2O	3.81	1.31	1.68	1.89
Si/Al	1.00	1.34	1.11	1.33
Loss on ignition, % (from TGA)	30.15	33.08	26.70	27.63

[a] CR — clay route.
[b] GR — gel route.

indicated during heating and a sudden increase is observed at 850–860°C for CR zeolites and at a slightly lower range for the GR ones.

3.3. Sintering of the ion exchanged zeolites

The products obtained by heating the ammonium zeolites at various temperatures were characterised by different methods. The XRD analysis of the CR zeolites show that the zeolite structure remains intact at 750°C whereas the products at 850°C are totally amorphous. At 950°C, mullite starts crystallising and remains as the only crystalline phase in the matrix at 1050 and 1150°C. In the case of zeolite NH_4A, maximum crystallinity is observed for the product at 1050°C whereas for NH_4X, the product at 1150°C is more crystalline. Figs. 2 and 3 represent the XRD patterns of fired products of selected zeolites NH_4A and NH_4X. The structure is lost at 750°C and the product at 850°C also remains amorphous for the GR zeolites. At higher temperatures 950, 1050 and 1150°C, the patterns remain similar to the products from the corresponding CR zeolites. However, some amount of amorphous phase appears to be present in all the products.

The values for water absorption, shrinkage and apparent density of the fired products from CR zeolites NH_4A, NH_4X, GR zeolites NH_4A and NH_4X are plotted against the temperature of firing and are shown in the Fig. 4a–d respectively. Zero water absorption is achieved for NH_4X zeolites at 1050°C whereas higher temperature (1150°C) was required for zeolite NH_4A. The shrinkage values also fall in a similar line i.e. the higher the water absorption the lower is the shrinkage. Apparent density of ~2.5 is achieved by all the zeolites when fired at 1150°C.

The compressive strength and true density of the sintered products are shown in Fig. 5. The GR zeolite NH_4X fired at 1050°C is found to have the maximum strength. The values for the CR zeolite NH_4X fired at 950, 1050 and 1150°C are almost close to each other unlike those of other products. For all the samples except GR zeolite NH_4A, the compressive strength is maximum for samples fired at 1050°C. The true density

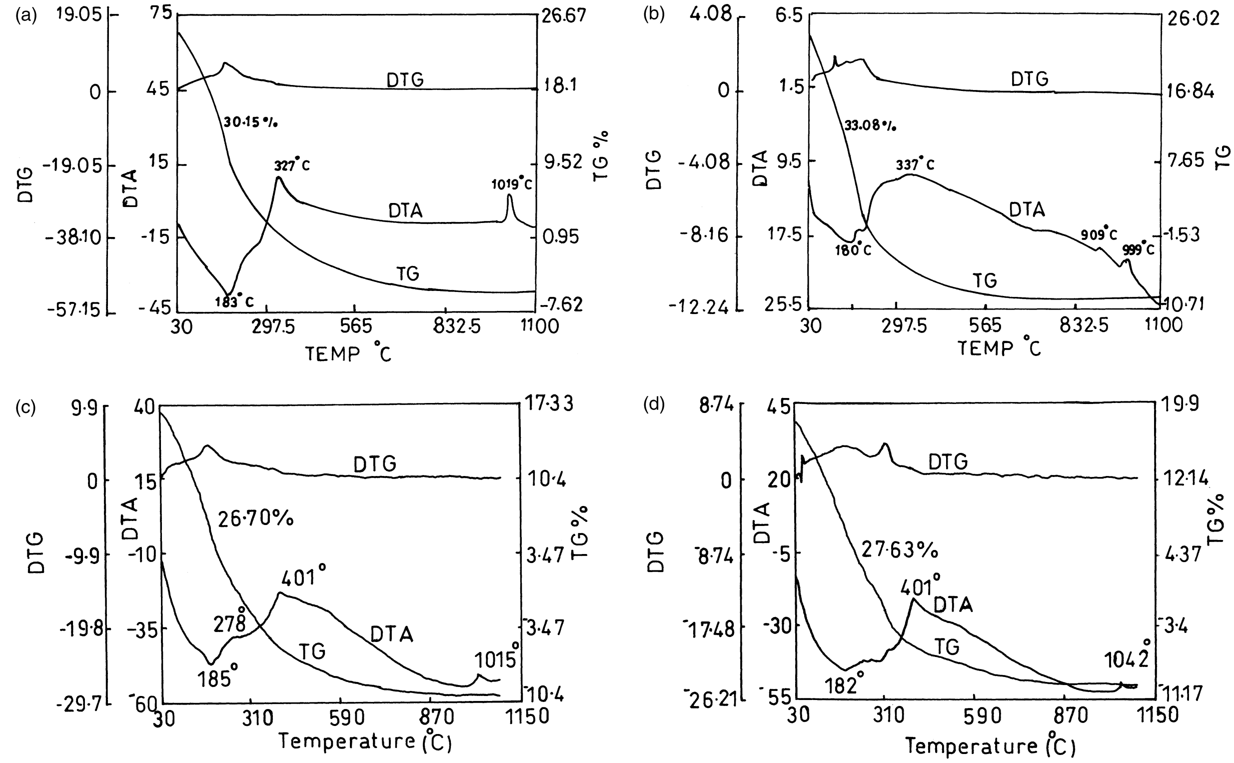

Fig. 1. DTA/TGA curves of the CR zeolites (a) NH_4A and (b) NH_4X. TA/TGA curves of the GR zeolites (c) NH_4A and (d) NH_4X.

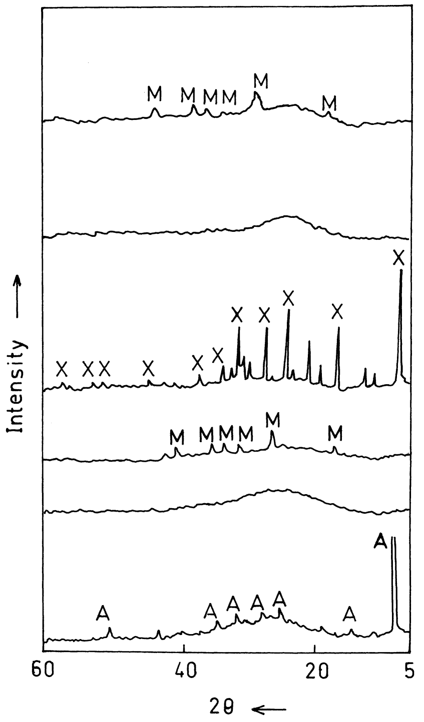

Fig. 2. XRD patterns of CR NH4 zeolites fired at different temperatures. (a) NH_4A 750°C; (b) NH_4A 850°C; (c) NH_4A 950°C; (d) NH_4X 750°C; (e) NH_4X 850°C and (f) NH_4X 950°C. A — Zeolite Na*A*; X — Zeolite Na*X*; M — Mullite.

values of the samples fired at 950°C are higher than the corresponding apparent densities whereas they come quite close for samples fired at higher temperatures.

The dielectric constant, resistivity and dielectric loss values at 1 MHz for the sintered products from the NH_4 zeolites are given in Table 3. The origin of the zeolites seems to have very little influence on the dielectric values.

Electron microscopic studies were conducted to examine the morphology of the fractured surfaces of the samples fired at 750, 850 and 1050°C and Figs. 6 and 7 give the photographs of products from CR zeolites NH_4A and NH_4X respectively. Zeolite Na*A* particles are reported to have bevelled cubic structure and zeolite Na*X* has typical octahedral geometry [1]. Multiple crystal growth is observed in both the zeolites. The ammonium exchange and heating at 750°C for 3 h appear to have little influence on the shape of the zeolite particles as shown by Figs. 6a and 7a. The porous nature of the material is clearly shown in the pictures. Heating at 850°C for 3 h results in the loss of particle shape in both the zeolites. Initiation of sintering is also indicated by smoothening of the surfaces and reduction in the porous sites (Figs. 6b and 7b). When the samples are heated at 1050°C, more glassy phase is formed with some crystalline particles embedded on to it as shown in Figs. 6c and 7c. Both the zeolites NH_4A and NH_4X behave in a similar manner. When the GR zeolites are fired at 750°C, the zeolite structure breaks down with some initiation of sintering as shown in Figs. 8a and b the SEM pictures of the zeolites NH_4A and NH_4X respectively.

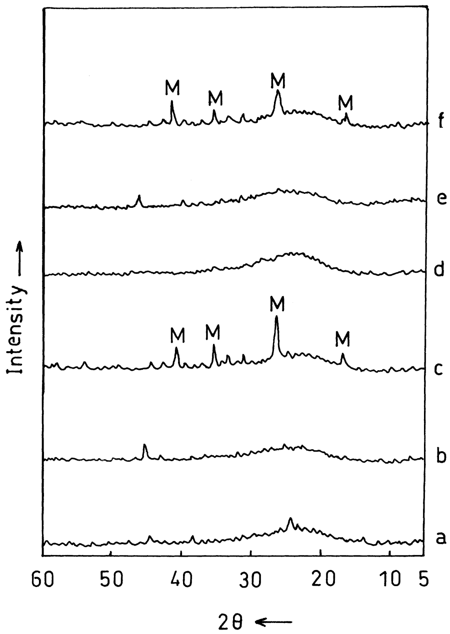

Fig. 3. XRD patterns of GR NH_4 zeolites fired at different temperatures. (a) NH_4A 750°C; (b) NH_4A 850°C; (c) NH_4A 950°C; (d) NH_4X 750°C; (e) NH_4X 850°C and (f) NH_4X 950°C; A — Zeolite Na*A*; X — Zeolite Na*X*; M — Mullite.

4. Discussion

The kaolin-based zeolites have certain fundamental differences from those prepared by the conventional gel route. Even the processed kaolin contains trace impurity minerals of iron, titanium, calcium, magnesium, etc. which are mostly retained in the zeolites, sometimes in different chemical forms. These elements may have some influence on the zeolite properties.

Particle size distribution of the GR zeolites is highly uniform whereas that of the CR zeolites is mostly dependent on the particle size of the metakaolin and also the synthesis conditions such as alkali/water ratio, stirring speed, etc. The particle size distribution of the metakaolin show ~63% particles below the 2 μm compared to ~80% in the kaolin. During the present investigation, the CR zeolite Na*A* was prepared under stirred condition and hence has a narrow size distribution. The CR zeolite Na*X* was synthesised under static conditions by ageing for 24 h at room temperature and heating in an air oven for 15 h and a broad size distribution is observed. The synthesis of GR zeolites was also carried out under static conditions. For sintering and ceramic formation, the uniformity in particle size is reported to be more favourable [26]. The ion exchange may not affect the size distribution. However, in the present

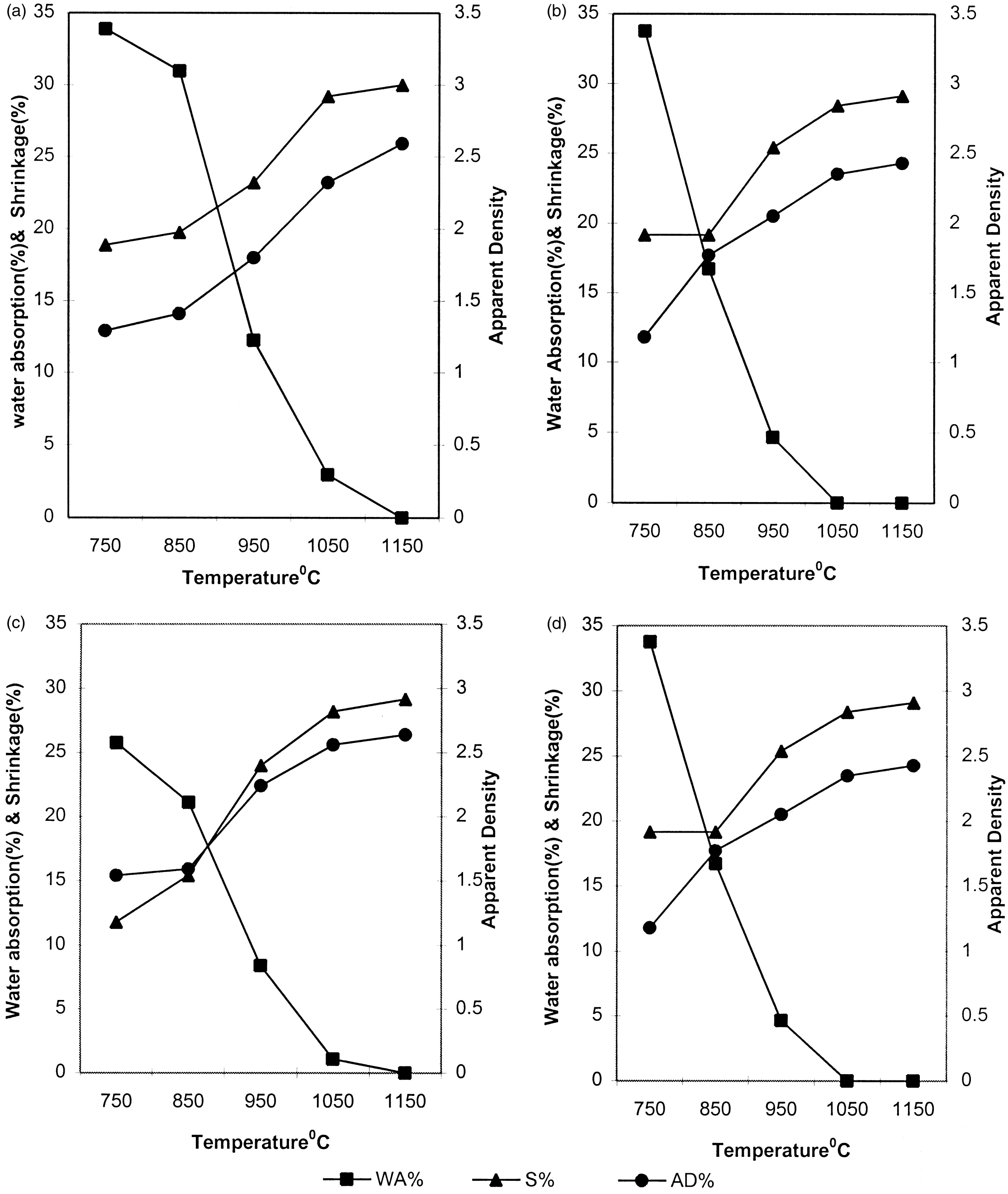

Fig. 4. Changes in properties of NH_4 zeolites fired at different temperatures. (a) CR NH_4A; (b) CR NH_4X; (c) GR NH_4A and (d) GR NH_4X.

investigation, CR zeolite NH_4X with a wide range of particles was found to sinter at a lower temperature compared to CR zeolite NH_4A having a narrow particle size distribution. The reason may be due to the excess silica which plays a dominant role in the sintering behaviour. This is further supported by the fact that in spite of having similar particle size distribution, the GR zeolite NH_4X is found to sinter at a lower temperature than the corresponding NH_4A zeolite. The water absorption values of the sintered products indicate the extent of sintering which in turn is related to hermeticity.

The ammonium exchange of the zeolites do not bring any change in the structure because the replacement of sodium ions by ammonium is taking place at the atomic level. This results in the uniform distribution of NH_4 ions in the zeolite structure. All the chemical constituents except sodium remain almost the same before and after the ion exchange as indicated by the chemical analysis results.

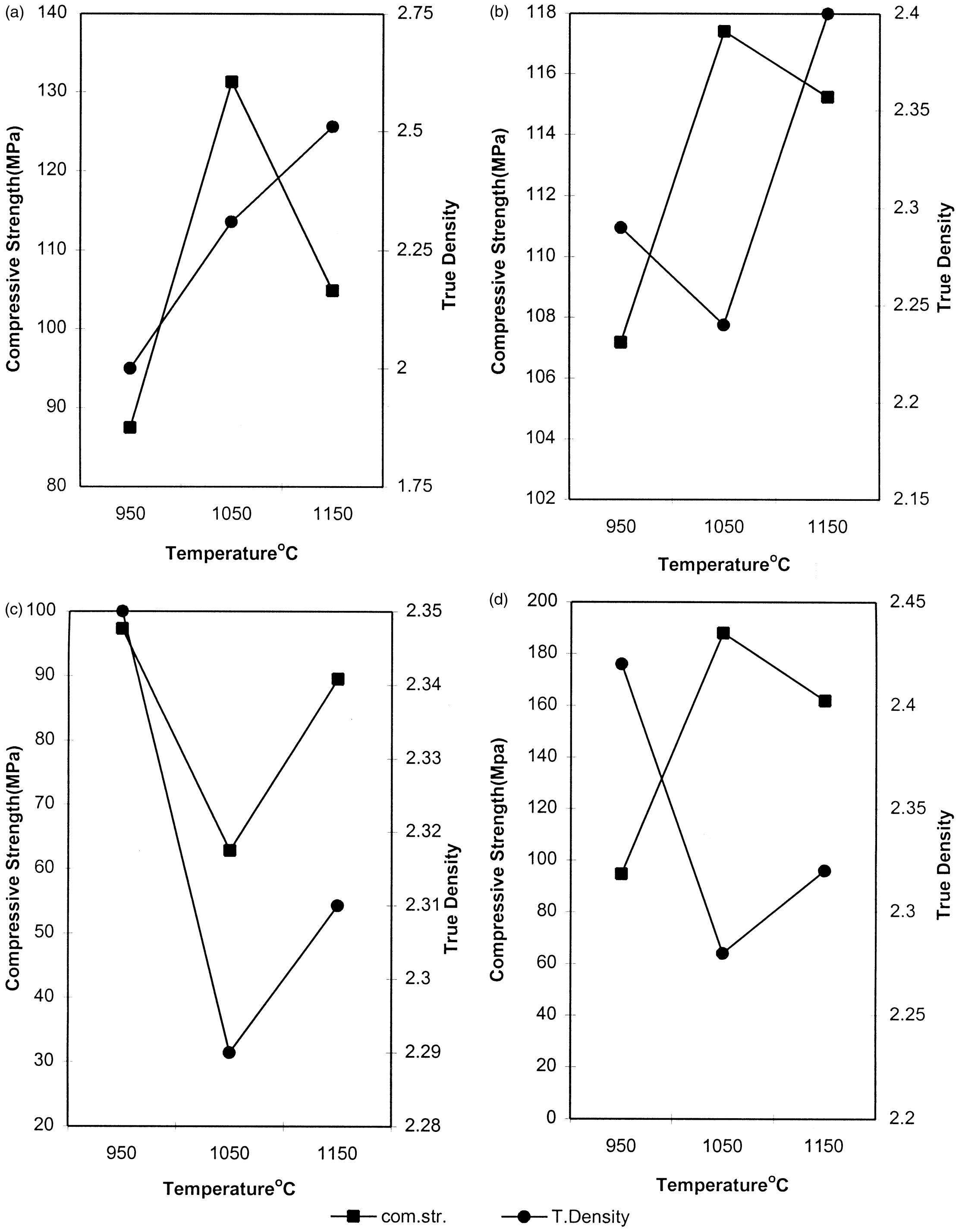

Fig. 5. Changes in properties of NH_4 zeolites fired at different temperatures. (a) CR NH_4A; (b) CR NH_4X; (c) GR NH_4A and (d) GR NH_4X.

The high weight loss of the NH_4 zeolites during heating as shown in the TG patterns can be attributed to the combined loss of water and ammonia. The weight loss in the sodium zeolites (Table 1) corresponds to the water loss only. The DTA gives information regarding the temperature of dehydroxylation, deammoniation, structural breakdown/amorphisation and formation of new phases. The endotherms at 150–180°C correspond to the loss of water whereas those at 330–400°C is attributed to the loss of ammonia [27]. The exotherms at the range 995–1018°C for the zeolites indicate the formation of mullite and glass phases. The additional small exotherm at 910°C in CR zeolite NH_4X can be due to the early sintering which is supported by the lower temperature of the exotherm at ~995°C (compared to 1018°C for CR zeolite NH_4A). The higher silica content

Table 3
Electrical properties of the NH_4 exchanged zeolites

	Zeolite	Temperature of firing (°C)	Dielectric constant (K)	Volume resistivity ($\times 10^4$ Ω.cm)	Loss factor (tan ∂)
CR[a]	NH_4A[c]	850	4.38	7.74	0.0804
		950	6.11	1.87	0.0627
		1050	4.19	4.53	0.1078
	NH_4X[d]	850	2.07	9.05	0.1005
		950	8.05	2.39	0.1062
		1050	4.42	5.05	0.1230
GR[b]	NH_4A	850	4.38	17.68	0.4213
		950	3.27	8.54	0.1539
		1050	3.37	5.71	0.1065
	NH_4X	850	3.72	12.30	0.2482
		950	3.38	9.98	0.1843
		1050	4.26	9.17	0.2186

[a] CR — clay route.
[b] GR — gel route.
[c] NH_4A — NH_4 zeolite A.
[d] NH_4X — NH_4 zeolite X.

in the former may contributing to this property [15]. In the corresponding GR zeolites, the exotherms were found at higher temperatures (1015°C for NH_4A and 1042°C for NH_4X). The sudden shrinkage in the TMA curves at ~860°C confirms the breakdown of zeolite structure and initiation of sintering as indicated by the X-ray amorphous nature of the sample fired at 850°C.

The sintering studies of the ammonium exchanged zeolites indicate that some amount of amorphous material remains in all the fired products. The zeolite structure is not much affected in the CR zeolites at 750°C whereas structural breakdown is observed for the GR zeolites at this temperature. But the formation of crystalline phases is observed at a lower temperature for the former. The presence of TiO_2, Fe_2O_3 etc. in the CR zeolites may be the reason for this behaviour. The effect of TiO_2 on the sintering of alumina has been reported by Hwang et al. [28]. They have observed promoting and retarding effects which depend on the amount of TiO_2 as well as the sintering temperature. The promoting effect of TiO_2 in the sintering of Al_2O_3 is also discussed by Das [29]. In the present system, the TiO_2 and Fe_2O_3 appears to retard sintering at 750°C as indicated by the stability of the CR zeolite structure. At higher temperatures i.e. >900°C, the sintering is favoured. Matsumoto has reported that structure of NH_4A zeolite breaks down at ~300°C [16] which does not match with other reports on the same. However, his observation that mullite crystallised directly from the amorphous state at ~950°C without formation of any intermediate spinel phase agrees with our findings. The formation of glassy phase and thereby sealing of the pores is achieved by both CR and GR zeolites NH_4X at a lower temperature as evident from the water absorption values. Most of the mullite particles formed at higher temperatures are getting covered by the flow of the glassy phase. The densification by viscous flow resulting in sintering is clearly indicated in the electron micrographs. The decrease in compressive strength for the products fired at 1150°C may be due to the increased glass formation.

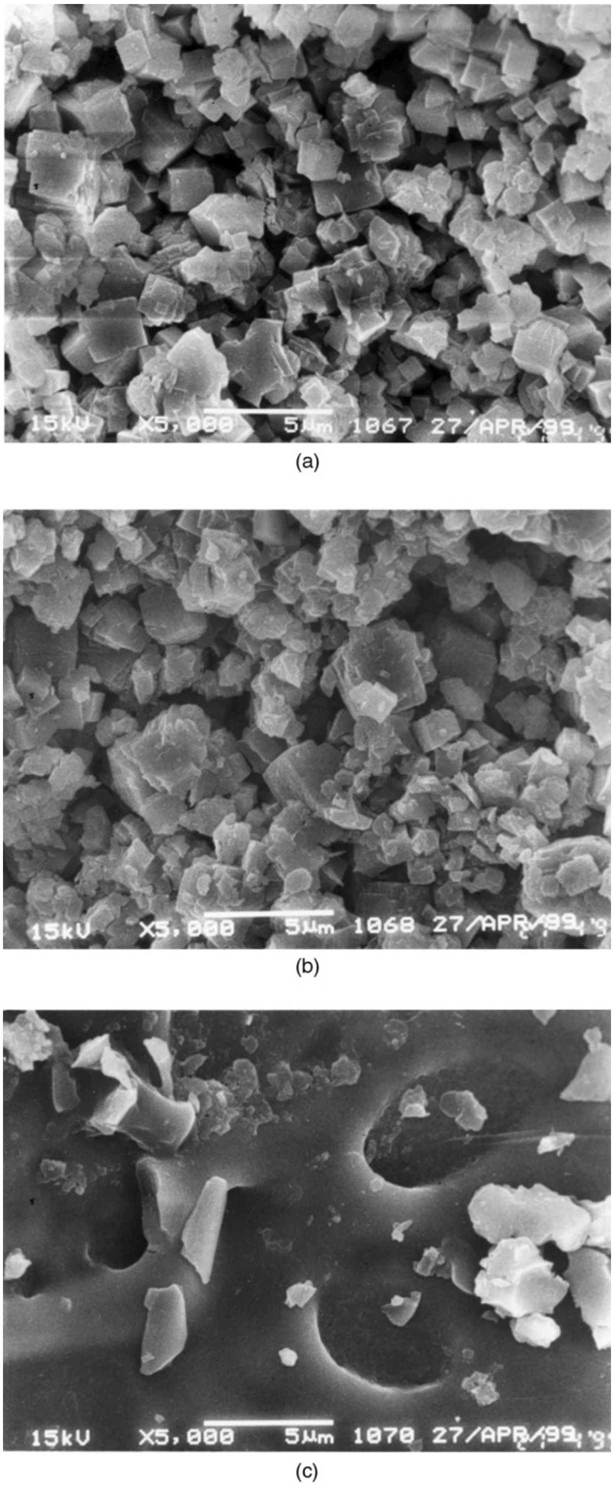

(a)

(b)

(c)

Fig. 6. SEM photographs of the fractured surfaces of sintered CR zeolites. (a) NH_4A 750°C; (b) NH_4A 850°C and (c) NH_4A 1050°C.

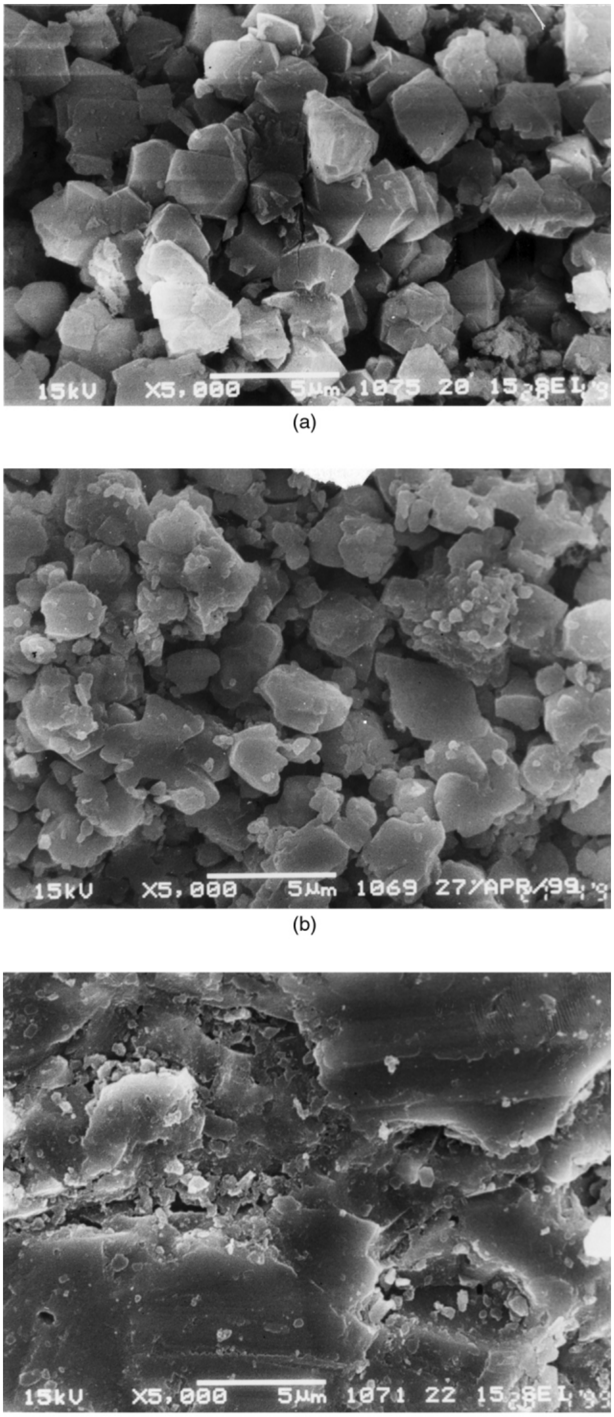

Fig. 7. SEM photographs of the fractured surfaces of sintered CR zeolites. (a) NH_4X 750°C; (b) NH_4X 850°C and (c) NH_4X 1050°C.

The peak heights in the XRD patterns indicate that more quantity of mullite is formed from NH_4A which is expected from the greater alumina content in the same (Table 2).

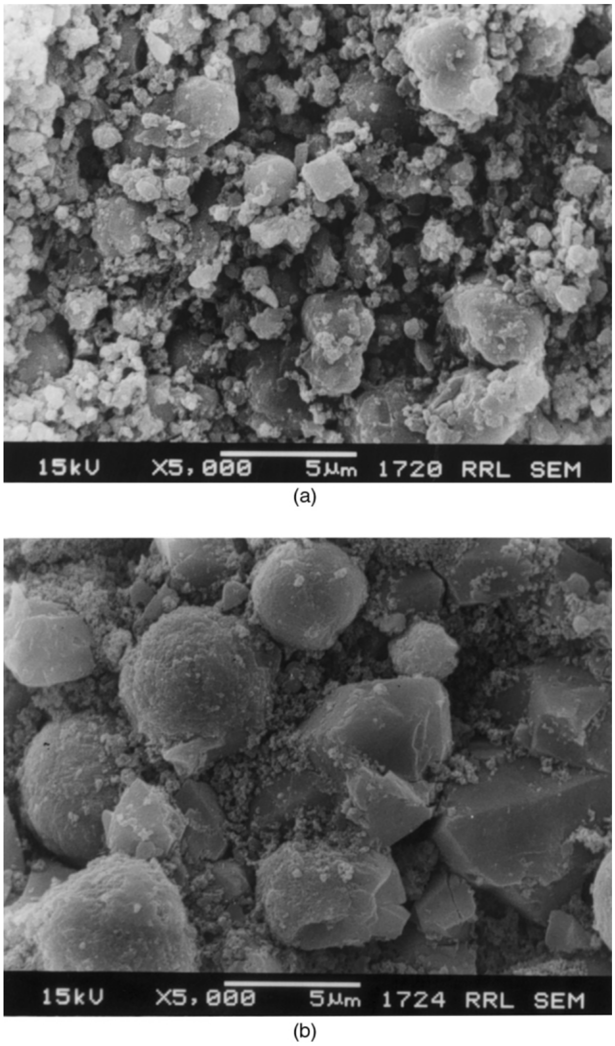

Fig. 8. SEM photographs of the fractured surfaces of sintered GR zeolites. (a) NH_4A 750°C and (b) NH_4X 750°C.

Synthesis of mullite by various methods has been reported in a number of publications [30–34]. In the present study, the sintered product is found to be a composite of fused glass and mullite particles. The density and compressive strength of this composite are found to be lower than those reported for pure mullite synthesised by conventional methods [35]. The compressive strength values more or less correspond to those of glass ceramics such as spodumene glass (140 MPa) and borosilicate glass (70 MPa) and is less than that of Al_2O_3 (280 MPa) [36].

The property requirement of substrate materials for microelectronic packaging and the properties of various aluminosilicate ceramics from zeolites which can probably be used as substrate materials are discussed by Subramanian et al. [35]. Mullite is reported to have a dielectric constant 6.6. The lower values for the sintered products containing mullite under the present study can be attributed to the presence of glassy phase along with crystalline mullite. However, the dielectric loss factors for the samples are quite high and the volume resistivity is not upto the mark for use in electronic ceramics. The clay based products were found to be inferior to the gel route products which can be due to the presence of impurities in the former.

5. Conclusions

(i) The zeolites Na*A* and Na*X* synthesised from kaolin contain most of the Fe_2O_3 and TiO_2 originally present in the clay whereas the gel route zeolites have very low content of the same.
(ii) These zeolites on exchange with ammonium ions give products with very low sodium content and the zeolite structure is not lost during ion exchange.
(iii) On heating, the ammonium exchanged GR zeolites were found to lose their crystallinity at a lower temperature compared to the corresponding CR zeolites. Further heating results in the formation of glass and crystallisation of mullite at a lower temperature in case of CR zeolites. The presence of Fe and Ti oxides seems to be responsible for this behaviour. The final product of sintering in both cases was found to be a mullite-glass composite material.
(v) The zeolite NH_4X with a higher Si/Al ratio than that NH_4A is found to get sintered a lower temperature irrespective of the synthesis route for the zeolite.
(iv) The sintered products were found to be inferior in strength to mullite prepared by conventional methods, but acceptable for substrate materials. The dielectric loss factor and volume resistivity were inferior to the acceptable values.

Acknowledgements

The authors are grateful to the Director, Regional Research Laboratory, Thiruvananthapuram (RRL, T) for permitting to communicate this work. Thanks are also due to Dr. U. Syamaprasad, Dr. Peter Koshy and Mr. P. Mukundan of RRL, T for providing the XRD, SEM and Thermal Analysis data respectively. Co-operation from Mr. P. Raghavan, Mrs. Vijaya Prasad and members of the Clay Group during this work is also gratefully acknowledged. Above all, one of the authors (PNP) is indebted to CSIR (Govt of India) for financial assistance.

References

[1] D.W. Breck, Zeolite Molecular Sieves: Structure, Chemistry and Uses, Wiley, New York, 1974.
[2] U. Choudhary, D.R. Corbin, M.A. Subramanian, (E.I.Du Pont de Nemours and company, Wilmington, Del.), US Patent 4 814 303, 21 March 1989.
[3] R.L. Bedard, E.M. Flanigen, (UOP, Des Plaines IL), US Patent 4 980 323, 25 December 1990.
[4] R.L. Bedard, E.M. Flanigen, (UOP, Des Plaines IL), US Patent 5 064 790, 12 November 1991.
[5] R.L. Bedard, E.M. Flanigen, (UOP, Des Plaines IL), Patent 5 071 801, 10 December 1991.
[6] R.L. Bedard, E.M. Flanigen, (UOP, Des Plaines IL), US Patent 5 179 051, 12 January 1993.
[7] R.L. Bedard, E.M. Flanigen, (UOP, Des Plaines IL), US Patent 5 192 722, 9 March 1993.
[8] G. Taga, M. Noritake, M. Enokuchi, (Tokuyama Soda Kabushiki Kaisha, JP), US Patent 5 166 107, 24 November 1992.
[9] G. Taga, M. Noritake, M. Nakamura, H.M. Zhang, (Tokuyama Soda Kabushiki Kaisha, JP), US Patent 5 036 030, 30 July 1991.
[10] C. Pareira, (United States, Washington, DC), US Patent 5 875 407, 23 February 1999.
[11] B. Hoghooghi, J. Mckittrick, E. Helsel, O.A. Lopez, Microstructural development, densification and hot pressing of celsian ceramic from ion-exchanged zeolite precursors, J. Am. Ceram. Soc. 81 (4) (1998) 845–852.
[12] B. Rudinger, R.X. Fischer, Phase formation in the sinter process of cordierite/mullite ceramics from Mg-exchanged zeolites A, P and X, in: H.G. Karge, J. Weitkamp (Eds.), Zeolite Science 1994, Recent Progress and Discussions, Studies in Surface Science and Catalysis, vol. 98, Elsevier, Amsterdam, 1995, pp. 283–284.
[13] K. Selvaraj, V. Ramaswamy, A.V. Ramaswamy, A novel route, using zeolites as the precursors, for the preparation of electronic ceramics, cordierite and β-spodumene and their characterisation, in: T.S.R. Prasada Rao, G. Muralidhar (Eds.), Recent Advances in Basic and Applied Aspects of Industrial Catalysis, Studies in Surface Science and Catalysis, vol. 113, Elsevier, Amsterdam, 1998, pp. 623–630.
[14] M.A. Subramanian, D.R. Corbin, U. Choudhry, Zeolites as precursors to aluminosilicate based ceramics for microelectronic packaging. Advances in Ceramics, The American Ceramic Society Publication 26 (1989) 239–247.
[15] Y. Kobayashi, E. Kato, Low temperature fabrication of anorthite ceramics, J. Am. Ceram. Soc. 77 (3) (1994) 833–834.
[16] T. Matsumoto, Y. Goto, K. Urbe, Formation process of mullite from NH_4^+-exchanged zeolite A, J. Ceram. Soc. Jpn 103 (1) (1995) 93–95.
[17] S. Chandrasekhar, P.N. Pramada, Sintering behaviour of calcium exchanged low silica zeolites synthesised from kaolin, Ceram. Int., 27 (2001) 105–114.
[18] S. Chandrasekhar, P. Raghavan, M. Lalithambika, Development of an indigenous technology for the production of detergent builder zeolite 4A from china clay. Lalithambika, Proceedings of the 6th Kerala Science Congress 1994, pp. 452–454.
[19] S. Chandrasekhar, P.N. Pramada, Investigation on the synthesis of zeolite NaX from Kerala kaolin, J. Porous Mater. 6 (1999) 283–297.
[20] L.V.C. Rees, S. Chandrasekhar, Formation of zeolite from the system Na_2O–Al_2O_3–SiO_2–H_2O in alkaline medium ($pH > 10$), Zeolites 13 (1993) 524–533.
[21] V.C. Mole, PhD thesis, University of London, 1989.
[22] H. Bennett, R.A. Reed, Chemical Methods of Silicate Analysis Academic Press, London, 1971.
[23] American Standards for Testing Materials, C 373, 1972.
[24] American Standards for Testing Materials, C 773, 1974.
[25] Roland von Ballmoos, Collection of Simulated XRD Powder Patterns for Zeolites, Butterworth on behalf of the Structure Commission of the International Zeolite Association, UK, 1984.
[26] E.M. Rabinowich, Review—preparation of glass by sintering, J. Mater. Sci. 20 (1985) 4259–4297.
[27] Wesley W.M. Wendladt, Thermal Analysis, Chemical Analysis, 0069-2883, vol. 19, Wiley, New York, 1986, p. 396.
[28] Chii-shyang Hwang, Zenbe-e Nakagawa, Tae-Hyun Sung, Yutaka Ohya, Kenya Haman, Report of the research laboratory of engineering materials, Tokyo Institute of Technology, 12 November 1987, pp. 93–102.

[29] A.R. Das, Densification of ceramics — Sintering and grain growth, in: D. Ganguli, S. Kumar (Eds.), Elements of Ceramic Science, vol. 2, Indian Institute of Ceramics, Calcutta, 1984, pp. 46–52.

[30] S. Kanzaki, H. Tabata, T. Kumazawa, S. Ohta, Sintering and mechanical properties of stoichiometric mullite, J. Am. Ceram. Soc. 68 (1) (1985) C6–C7.

[31] S. Somiya, Y. Hirata, Mullite powder technology and applications in Japan, Ceram. Bull. 70 (10) (1991) 1624–1632.

[32] A.K. Chakravorty, D.K. Ghosh, Synthesis and 980°C phase development of some mullite gels, J. Am. Ceram. Soc. 71 (11) (1988) 978–987.

[33] S. Wu, N. Claussen, Fabrication and properties of low-shrinkage reaction bonded mullite, J. Am. Ceram. Soc. 74 (10) (1991) 2460–2463.

[34] J.A. Pask, A.P. Tomsia, Formation of mullite from sol–gel mixtures and kaolinite, J. Am. Ceram. Soc. 74 (10) (1991) 2367.

[35] M.A. Subramanian, D.R. Corbin, U. Choudhry, Better ceramic substrates through zeolites, Bull. Mater. Sci. 16 (6) (1993) 665–678.

[36] J.V. Knickerbocker, Over view of the glass-ceramic copper substrate — a high performance multilayer package for the 1990s, Am. Ceram. Soc. Bull. 71 (9) (Sept 1992).